Earth and Planetary Science Letters 440 (2016) 115–126

Contents lists available at ScienceDirect

Earth and Planetary Science Letters

www.elsevier.com/locate/epsl

Fast rupture propagation for large strike-slip earthquakes

Dun Wang [a,*], Jim Mori [b], Kazuki Koketsu [a]

[a] Earthquake Research Institute, University of Tokyo, 1-1-1, Yayoi, Bunkyo-ku, Tokyo 113-0032, Japan
[b] Disaster Prevention Research Institute, Kyoto University, Uji, Kyoto 611-0011, Japan

ARTICLE INFO

Article history:
Received 13 August 2015
Received in revised form 10 February 2016
Accepted 11 February 2016
Available online 23 February 2016
Editor: P. Shearer

Keywords:
rupture speed
seismic array
back-projection
supershear rupture

ABSTRACT

Studying rupture speeds of shallow earthquakes is of broad interest because it has a large effect on the strong near-field shaking that causes damage during earthquakes, and it is an important parameter that reflects stress levels and energy on a slipping fault. However, resolving rupture speed is difficult in standard waveform inversion methods due to limited near-field observations and the tradeoff between rupture speed and fault size for teleseismic observations.

Here we applied back-projection methods to estimate the rupture speeds of 15 $M_w \geq 7.8$ dip-slip and 8 $M_w \geq 7.5$ strike-slip earthquakes for which direct P waves are well recorded in Japan on Hi-net, or in North America on USArray. We found that all strike-slip events had very fast average rupture speeds of 3.0–5.0 km/s, which are near or greater than the local shear wave velocity (supershear). These values are faster than for thrust and normal faulting earthquakes that generally rupture with speeds of 1.0–3.0 km/s.

1. Introduction

Large earthquakes nucleate from a small area in the hypocentral region, then expand over the fault plane. Rupture speed is a parameter that describes how fast the rupture front expands. This is a key observation for understanding the controlling stresses, friction, and damage during an earthquake, yet the speed and its variations are usually difficult to determine. There are many open questions related to rupture speed. For example, are there differences between dip-slip and strike-slip earthquakes? How common are supershear ruptures during large earthquakes? Theoretical and experimental research indicates that faulting during strike-slip earthquakes can propagate faster than the local S wave velocity (supershear rupture), but this phenomenon has been observed or inferred for only a small number of events (Archuleta, 1984; Bouchon et al., 2001; Bouchon and Vallee, 2003; Dunham and Archuleta, 2004; Ellsworth and Celebi, 1999; Ellsworth et al., 2004; Frankel, 2004; Robinson et al., 2006; Song et al., 2008; Vallée et al., 2008; Walker and Shearer, 2009; Wang and Mori, 2012; Wang et al., 2012; Yue et al., 2013; Zhan et al., 2014).

Using teleseismic waveforms, which are the only data available for many large earthquakes, there are difficulties for estimating the rupture speed with standard waveform inversions, due to trade-off between the rupture speed and fault size (e.g., Fan et al., 2014). Over the past ten years, however, back-projection methods using dense seismic arrays have been able to more accurately estimate the time and position of the high frequency radiation relative to the epicenter, which can be interpreted as the propagating rupture front (Ishii et al., 2005; Kruger and Ohrnberger, 2005). This study presents rupture speed estimates from back-projections for large earthquakes that were well recorded on large regional arrays in Japan and the US.

2. Data and method

We analyzed all recent $M_w \geq 7.5$ strike-slip and $M_w \geq 7.8$ dip-slip earthquakes during 2004–2013, for which epicenters were 30° to 85° from Hi-net (Okada et al., 2004) in Japan or USArray (www.usarray.org) in the continental US. The distance limitation was set according to the epicentral distances for which the direct P-wave could be recorded clearly (Fig. 1). Four large strike-slip earthquakes that occurred between 2001 and 2004, and one tsunami earthquake (2006 Java earthquake) that was analyzed using the same procedure in Wang (2013) was also included.

Back-projection methods are commonly used techniques that calculate time-shifted stacks of seismic waveforms to estimate the time and location of the sources of the seismic waves. They determine which points of a grid over the earthquake fault area are the sources of coherent seismic radiation in each designated time window of the P-wave across the recording network.

Motivated by and similar to Ishii et al. (2005) and Kruger and Ohrnberger (2005), we developed a back-projection scheme that is adapted from beamforming to image the source propagation of large earthquakes. Our approach is similar to beampacking

* Corresponding author.
E-mail address: dunwang@eri.u-tokyo.ac.jp (D. Wang).

http://dx.doi.org/10.1016/j.epsl.2016.02.022
0012-821X/

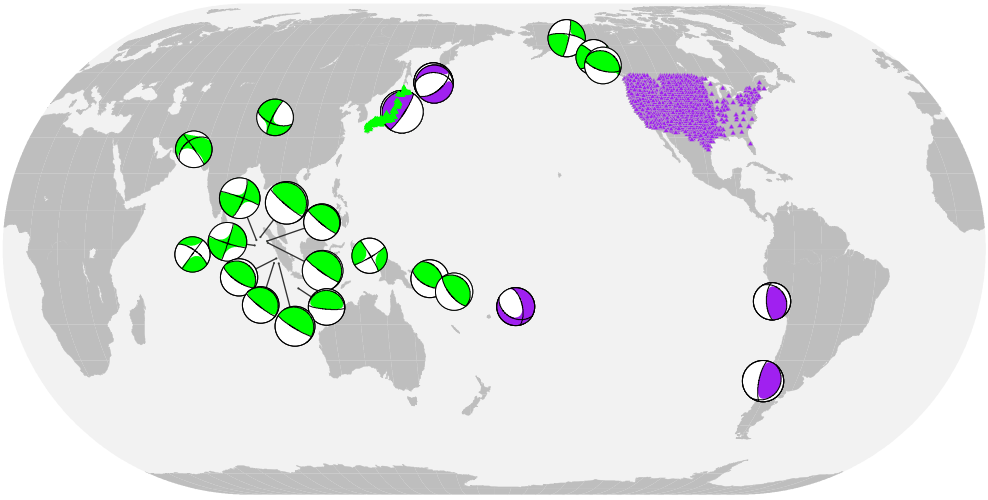

Fig. 1. Locations of earthquakes analyzed in this study. Green and purple triangles indicate Hi-net (774), and USArray (3257) stations, respectively. The focal mechanisms are obtained from the Global CMT Project, in which color indicates the data source (green for Hi-net and purple for USArray). (For interpretation of the references to color in this figure legend, the reader is referred to the web version of this article.)

(time domain wavenumber analysis) that beamforms over predefined grid points and measures the stacked power (Rost and Thomas, 2002; Schweitzer et al., 2002). Here we used the relative travel-time differences across the stations as calculated from the locations of the grid (source) points. In this way we account for the curvature of the wavefront rather than assuming a plane wave (i.e., a fixed slowness). We performed the beamforming over a sliding window to image the stacked energy corresponding to each grid point. Since the obtained time is the local beam time, a time correction is necessary to account for the varying travel times between the source locations and the station array. To avoid confusion with traditional back-projection (e.g., Ishii et al., 2005), which does not require a time correction, we call this approach sliding-window beampacking (hereafter referred to as our (back-projection) method).

Similar to Ishii et al. (2005), we first aligned all waveforms on the first arrival using waveform cross correlations, constraining the initial source location to the epicenter (usually determined by USGS, although for the 2011 Tohoku, Japan M_w 9.0 earthquake, the JMA location is used). For the alignment, we first cross correlated longer time windows (10 s of the initial arrival) of the onset in a relatively lower frequency band (0.01 to 0.5 Hz), and applied these obtained station corrections to the waveforms. Then, we cross correlated a second time using 6 s time windows (after the initial arrival) for higher frequency bands (1.0 to 10.0 Hz) with a small offset (0.5 s). This two-step procedure gives a good high-frequency station correction and avoids errors that may be caused by cycle slip in the higher frequencies. After correcting for stations, all times were relative to the initial onset time. Therefore, our back-projection procedure assumed that the onset of the waveform corresponds to the hypocenter of the earthquake. All subsequent spatial and temporal determinations of the high-frequency sources were relative to the hypocenter and onset time.

To obtain the locations of the sources of maximum radiation, we used 10 s time windows that were offset by 1 s. Time shifts for each station in the stack were calculated using the theoretical travel times from the station to the grid point, from the velocity structure IASPEI 1991 (Kennett, 1991).

We tested a series of frequency bands (0.5–1.0 Hz, 0.5–2.0 Hz, 0.8–8.0 Hz, and 1.0–10.0 Hz) for several earthquakes such as the 2001 Kunlun M_w 7.8 earthquake, and obtained similar patterns of ruptures among results. The rupture front likely produces more high frequency energy because of the initiation of brittle failure, so we used data band-pass filtered between 1.0 and 10.0 Hz for Hi-net and USArray.

We used our back-projection method for the events that have mainly unilateral ruptures. However, it was difficult to use the method for bilateral ruptures and more complicated earthquakes, such as the M_w 8.6 and M_w 8.2 off Sumatra earthquakes in 2012, which showed conjugate faulting on four or five faults for the larger one. Therefore a new inversion method previously developed by Wang et al. (2012), was used to identify the locations of multiple sources (the 2012 M_w 8.6 and M_w 8.2 off Sumatra earthquakes) in each time window using an empirical spatial function of the network response for a point source in the source region. The spatial response functions were obtained by back-projecting the first 10 s of the initial waveforms of the mainshocks. Then, this response function was deconvolved from the spatial pattern of stacked amplitudes for each time window in the back-projection. The deconvolution for the spatial response functions is done through a non-negative least-square inversion algorithm.

Since event times of the high-frequency sources were relative to the onset time, there needs to be a time correction. The source location (relative to the hypocenter) did not change, but the occurrence time (relative to the onset) needed to be adjusted for the azimuth between the rupture direction and the direction to the stations along with distance along the rupture. An array in the direction of the rupture would have earlier apparent source times (relative to the onset) than an array in the direction opposite of the rupture (Yao et al., 2011). For these large earthquakes, the general direction of rupture could be seen clearly from the spatial pattern of the back-projection results. This rupture duration at individual station can be described by the equation (Ni et al., 2005)

$$L/v_r = \delta t + L\cos(\theta)/V\,.$$

Here δt is the apparent source time at azimuth θ with respect to the rupture direction. L, v_r, V are the rupture length, rupture speed, and P wave apparent velocity at that epicenter distance, respectively. Therefore calculating the second term, using the azimuth and apparent velocity, will obtain the time correction for the results derived from back-projections. A geographically central location of the array stations is used for the time corrections for the point with maximum stacked amplitude in each time window.

Notice that the back-projected energy is smeared in time and space due to the finite length of the stacking window; it is thus hard to determine the end of rupture from the back-projected en-